# Nanoscale

Accepted Manuscript


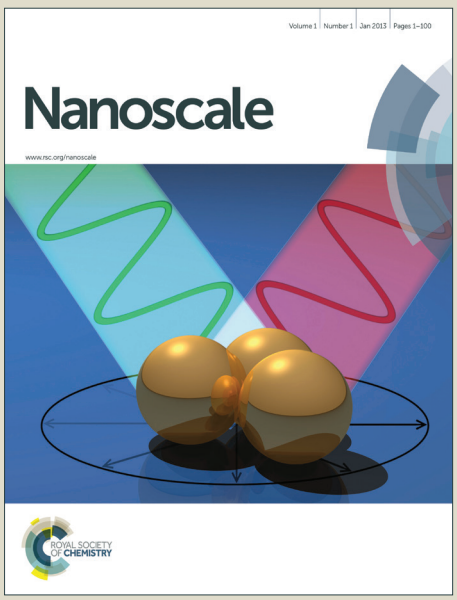





ROYAL SOCIETY OF CHEMISTRY

www.rsc.org/nanoscale

Journal Name

RSCPublishing

COMMUNICATION

Cite this: DOI: 10.1039/xoxxoooooox

# Hybrid atomic structure of the Schmid cluster $Au_{55}(PPh_3)_{12}Cl_6$ resolved by aberration-corrected STEM

Received ooth January 2012,
Accepted ooth January 2012

DOI: 10.1039/xoxxoooooox

www.rsc.org

Nan Jian[a], Christopher Stapelfeldt[b], Kuo-Juei Hu[a], Michael Fröba[b] and Richard E. Palmer*[a]

**Abstract**

**We have investigated the atomic structure of the $Au_{55}(PPh_3)_{12}Cl_6$ Schmid cluster by using aberration-corrected scanning transmission electron microscopy (STEM) combined with multislice simulation of STEM images. Atom counting was employed, with size-selected clusters as mass standards, to "fractionate" the correct cluster size in the image analysis. Systematic structure analysis shows that a hybrid structure, predicted by density functional theory, best matches nearly half the clusters observed. Most other clusters are amorphous. We believe our conclusions are consistent with all the previous, apparently contradictory structural studies of the Schmid cluster.**

The report of the ligand-stabilized $Au_{55}(PPh_3)_{12}Cl_6$ cluster by Schmid and colleagues in 1981[1] was a significant event in the emergence of nanotechnology. Its size (1.4nm), stability and electronic properties drew a great deal of attention.[2-12] It was quickly seen as the basis of a future single electron transistor and, more generally, a potential building block of a nanostructured system.[2-7]However, the atomic structure of $Au_{55}(PPh_3)_{12}Cl_6$ has long remained a mystery, not least because the cluster resisted the crystallization which is needed to allow single-crystal X-ray diffraction analysis.[13,15]

The first structure proposed for $Au_{55}(PPh_3)_{12}Cl_6$ came in the original Schmid work,[1] based on Mossbauer spectra. This showed 4 types of Au atoms, consistent with a cuboctahedral model (one example of a fcc structure). Later, in 1990, the Extended X-Ray Absorption Fine Structure (EXAFS) method was used to measure the average coordination number of Au atoms: the best match to that data was a cuboctahedron.[9,10] EXAFS, X-ray absorption near edge structure (XANES) and wide-angle X-ray scattering (WAXS) analyses of $Au_{55}(PPh_3)_{12}Cl_6$ followed in 2001 and also supported fcc structure.[11]

However, in parallel with this work, an icosahedral structure for $Au_{55}(PPh_3)_{12}Cl_6$ was first suggested in 1993 by Vogel et al: the diffraction curve of $Au_{55}(PPh_3)_{12}Cl_6$ powder best fitted the simulation of an icosahedron.[12] On the theory front, an ab initio investigation of $Au_{55}(PPh_3)_{12}Cl_6$ in 2010 agreed with the icosahedral assignment.[13] Beyond cuboctahedral and icosahedral proposals, Rapoport et al proposed (1997) that the $Au_{55}(PPh_3)_{12}Cl_6$ cluster was heterogeneous in structure, based on a combination of cryo high resolution transmission electron microscopy (HRTEM), X-ray scattering(XRS), analytical ultracentrifugation(AUC), thermogravimetriy and differential thermoanalysis (TG/DTA) measurements.[14] Other TEM studies[12,14,15] of $Au_{55}(PPh_3)_{12}Cl_6$ clusters were mainly focused on the measurement of cluster size: all showed a diameter of about 1.4nm. But the electron microscope was not used extensively for studying the atomic structure of $Au_{55}(PPh_3)_{12}Cl_6$, only a few images of clusters of uncertain size have been reported.[15]

Aberration-corrected scanning transmission electron microscopy (STEM) is a powerful and increasingly widespread method to investigate the atomic structure of nanomaterials.[16-23] In the high angle annular dark field (HAADF) mode of STEM, the signal collected is the electron flux scattered incoherently through high angles. The intensity of the atomic columns in the image depends on the number of atoms in each column and the atomic number.[23-28] This "Z contrast" method can significantly improve the visibility of heavy element clusters (in our case, gold) supported on light, thin substrates (eg. carbon) and also makes it possible the use of size-selected clusters as mass balances to determine the number of atoms in the specimen nanoparticle.[18, 29-33]

Our systematic experimental study of the atomic structure of $Au_{55}(PPh_3)_{12}Cl_6$ clusters, coupled with multislice simulations, reveals that a hybrid structure best matches about half the clusters, with a similar fraction found to be amorphous.[34,35] The hybrid structure, as predicted theoretically for the bare $Au_{55}$ cluster, contains both icosahedral and close-packed cubic structure elements. Thus our hybrid structure rationalises the preceding cuboctahedral

and icosahedral proposals,[1,9-13] while the amorphous fraction we also find is consistent with the preceding evidence of heterogeneity in the Schmid clusters.[14]

The $Au_{55}(PPh_3)_{12}Cl_6$ clusters were synthesised in Hamburg using the Schmid method[1]. The differential scanning calorimetry (DSC), powder X-ray diffraction (pXRD) and nuclear magntic resonance (NMR) analysis, presented in the supplementary information, show that the clusters are intact and the ligands are linked to the metal core. The clusters sent to Birmingham in powder form, and redissolved in dichloromethane and drop casting onto one half of a 400-mesh TEM grid covered with an amorphous carbon film. Size-selected $Au_{309}$ clusters were generated with a magnetron sputtering, gas condensation cluster beam source and mass selected with a lateral time-of-flight (TOF) mass selector.[36-38] These size-selected clusters were deposited onto the other half of the same TEM grid(the half grid on which the $Au_{55}(PPh_3)_{12}Cl_6$ clusters were subsequently deposited was covered by a cap to prevent the deposition of the $Au_{309}$ clusters, in case they affected the ligand-protected clusters.): the cluster beam current was 20pA and deposition time 150 seconds, the number of clusters deposited was ~$1.9x10^{10}$. Our 200kV JEOL 2100F STEM with Cs corrector (CEOS) was equipped with an HAADF detector operated with inner angle 62 mrad and outer angle 164 mrad. All the images were typically taken in less than 2.7 seconds (equal to two scanning times over the whole image area) and no beam shower has been employed to minimize the beam damage.[39]

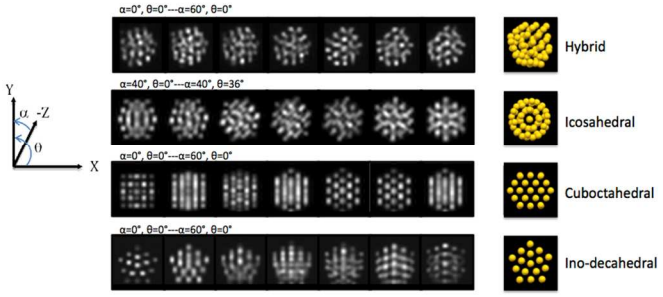


**Figure 1.** Examples from STEM simulation atlas of hybrid structure (from α=0°, θ=0° to α=0°, θ=0°) plus icosahedral (from α=40°, θ=0° to α=40°, θ=36°), cuboctahedral (from α=0°, θ=0° to α=60°, θ=0°) and Ino-decahedral (from α=0°, θ=0° to α=60°, θ=0°) structures

The QSTEM simulation software package[40] was utilized to relate the experimental STEM images to models of candidate atomic structures: Hybrid, icosahedral, cuboctahedral, and Ino-decahedral model structures. Examples of simulated images are shown in Figure 1. Since the clusters are deposited onto the carbon surface of the TEM grid in a random orientation, the STEM images show disparate patterns corresponding to clusters in different orientations. In the Figure 1, for example, the Ino-decahedral structure at (α=0°, θ=0°) shows a five-fold symmetry axis, but when tilting the atomic model 60° towards α, the simulated images show quite different features. Thus for a comprehensive investigation of the possible cluster structures, we employ a "simulation atlas",[41] a set of simulations across the whole range of cluster structure orientations, with which each experimental image is compared. (See Figure 1) To date, comparison is best conducted manually by classifying the simulation images according to the structural motifs they present, such as a ring, parallel lines, or a ring with central dot. Thus each experimental image is compared with the simulation images for every orientation of each candidate structure.

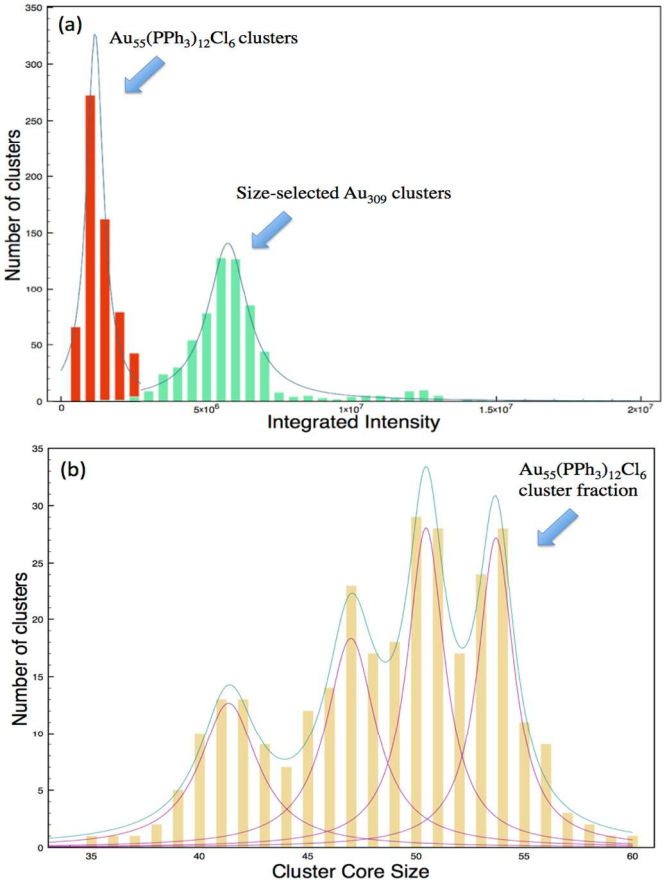


**Figure 2.** Weighing Schmid clusters against size-selected clusters. (a) The HAADF intensity of Schmid clusters (red) and size-selected $Au_{309}$ clusters (green). (b) Fine size distribution of Schmid clusters. The forth peak at an equivalent Au core size of 54±1.5 is assigned to $Au_{55}(PPh_3)_{12}Cl_6$ clusters.

Comparison of the STEM integrated intensity of each cluster prepared by the Schmid method with the size-selected $Au_{309}$ mass standards shows that there is some variation in the nuclearity of the "Schmid clusters" beyond that of pure $Au_{55}(PPh_3)_{12}Cl_6$. But the same comparative intensity measurement enable us to "fractionate" the chemically prepared sample to focus on the "$Au_{55}$" clusters which are of most interest. Figure 2(a) shows the relative intensities of the Schmid clusters and the size-selected $Au_{309}$ clusters. The ligands of a $Au_{55}(PPh_3)_{12}Cl_6$ cluster contribute an intensity equivalent to 9.88 Au atoms, based on previous calibration of our STEM.[42] After subtracting this ligand intensity, we obtain a mean value for the chemically synthesized Schmid clusters of 53.4 ± 3.2 Au atoms in the core. A high-resolution plot is given in Figure 2(b) and shows fine structure within this distribution, with 4 peaks appearing at 41±2, 47±1.5, 50±1.5 and 54±1.5 Au atoms. The peak at 54±1.5 is assigned to the $Au_{55}(PPh_3)_{12}Cl_6$ clusters and forms the focus of our subsequent atomic structure analysis.

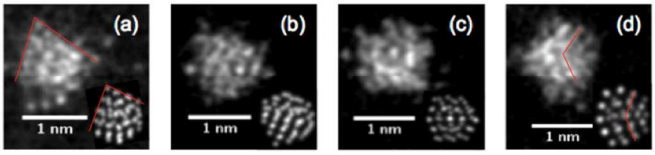


**Figure 3.** Typical high resolution HAADF-STEM images of $Au_{55}(PPh_3)_{12}Cl_6$ clusters which are assigned to have hybrid structure and orientations of (a) α=70°, θ=40°, (b) α=30°, θ=30°, (c) α=60°, θ=80° and (d) α=100°, θ=0°. The insets are the corresponding best matched simulated images.

Figure 3 shows examples of high resolution HAADF-STEM images of clusters corresponding to the "true $Au_{55}$" fraction of the synthesized Schmid clusters. These experimental image examples are illustrations of the 72 images obtained from this fraction. Based on the fit between the images and the simulate atlas, we find no match to the cuboctahedral, icosahedral and Ino-decahedral structures. All the 30 of 72 clusters best match the DFT predicted asymmetrical hybrid structure. For example, the cluster in Figure 3(d) shows a very similar pattern of parallel fold lines, with an angle of 122°, to the hybrid model STEM simulation image of orientation (α=100°, θ=0°), with a angle of 128°. The remaining 42 clusters of 72 clusters were justified to be amorphous.

Of course the simulations do not match the experimental data exactly. One reason is the effect of the electron beam, as reported in many previous studies on small clusters like $Au_{20}$, MP-$Au_{38}$, $Au_{40}(SR)_{24}$[41,43-45] which gives rise to atomic motion ("atom smearing") during image acquisition. A serial integrated intensity analysis of one cluster was employed to test whether the cluster dissociated under the electron beam. This is shown in Figure S4 of the SI. The experimental conditions are the same as the normal imaging of the clusters. Since there is no obvious change in the cluster's integrated intensity during the continuous scanning, we conclude that the electron beam does not lead to significant atom loss from the cluster under the experimental condition used, especially over the first few scans. Given that slight changes of the cluster structure is possible after repeated the electron beam, only STEM images obtained from the first or second scans were employed in the structure analysis. Such changes may also come about through purely thermal effects. Naturally the interaction between clusters and the amorphous carbon film substrate also creates the possibility of a "local" change of the cluster structure.[43]

The effect of ligands on the atomic structure of thiol monolayer-protected clusters is reported in many studies, eg of $Au_{102}$(p-MBA)$_{44}$ and $Au_{144}SR_{60}$.[46-49] The strong, covalent Au-S bond distorts the outer shell of the metal core and forms a quite different structure from the inner core. However, for the $Au_{55}(PPh_3)_{12}Cl_6$ cluster, the phosphine ligands are weakly band and their effect on the structure is expected to be very much less significant.[3] So the structure of metal core should not be affected too much. This explains why the metal core structure of the ligand-protected $Au_{55}(PPh_3)_{12}Cl_6$ clusters fits the hybrid isomer of bare $Au_{55}$ very well. Even loss of some ligands from the gold core investigated here due to adsorptions, drying or the electron beam should not significantly distort the core structure.

Can we rationalize our proposed assignment for $Au_{55}(PPh_3)_{12}Cl_6$ as a mixture of the hybrid isomer and amorphous structures with the previous, contradictory assignments of cuboctahedral or icosahedral structure. First, the hybrid structure was not proposed (for bare $Au_{55}$ clusters) till 1998 and has never previously been considered as a candidate for the Schmid cluster.[34] Secondly, the hybrid structure is seen to contain structural elements characteristic of both the icosahedron and the cuboctahedron. As the Figure 3(b) shows, this hybrid isomer resembles, colloquially speaking, a close-packed plane "bolted on" to terminate an icosahedral cluster. This hybrid nature may then explain the cubic type feature found in EXAFS analysis[9-11] and the icosahedral-type diffraction peak found in X-ray diffraction research.[12] Moreover, the average coordination number of the hybrid model (7.78) closely resembles the coordination number of the cuboctahedral (7.85), and the previous EXAFS researches measured the average coordination numbers (7.8±1[9] and 7.3±2.5[10]) are also support this hybrid model.

## Conclusions

In conclusion, we find that the Schmid synthetic route does produce passivated clusters consistent with the formula $Au_{55}(PPh_3)_{12}Cl_6$ clusters as well as clusters containing from about 35 to 60 Au atoms. The fraction of clusters containing 54±1.5 Au atoms, as fractionated by the cluster "mass balance" (and assuming the standard ligand number), presents atomic structures, measured by aberration corrected STEM which fit best to the hybrid model (42%) and amorphous structures (58%). We found no evidence of the previously proposed cuboctahedral and icosahedral structures. However the hybrid structure, first proposed for bare $Au_{55}$, contains both close-packed and icosahedral-type motifs and appears to rationalize the previous contradictory assignments. Looking forward, the combination of size-fractionation by the STEM mass balance method and atomic structure determination in the aberration-correction regime holds promise to reveal the isomeric structures of other nanoparticles.

## Acknowledgements

We thank Dr. Simon Plant for deposition of the size-selected gold clusters. We thank Professor Ignacio Garzon for providing the atomic hybrid model. We acknowledge financial support from the EPSRC and TSB. The STEM instrume,m nt employed in this research was obtained through the Birmingham Science City project "Creating and Characterising Next Generation Advanced Materials," supported by Advantage West Midlands (AWM) and in part funded by the European Regional Development Fund (ERDF).

## Notes and references

[a] Nanoscale Physics Research Laboratory, School of Physics And Astronomy, University of Birmingham, Birmingham, B15 2TT, UK

[b] Institute of Inorganic and Applied Chemistry, Department of Chemistry, University of Hamburg, D-20146, Hamburg, Germany

Corresponding Author:
Richard E. Palmer,
Email: R.E.Palmer@bham.ac.uk

### References

1. G. Schmid, R. Pfeil, R. Boese, Chem. BER 1981, 114, 3634.
2. G. Schmid, L. F. Chi, Adv. Mater. 1998, 10, 515.
3. G. Schmid, Chem. Soc. Rev. 2008, 37, 1909.
4. L. Chi, M. Hartig, T. Drechsler, T. Schwaack, C. Seidel, H. Fuchs, G. Schmid, Appl. Phys. A Mater. Sci. Process. 1998, 190, 187.

5. G. Schmid, M. Bäumle, M. Geerkens, I. Heim, C. Osemann, T. Sawitowski, Chem. Soc. Rev. 1999, 28, 179.
6. G. Schmid, Y. Liu, M. Schumann, Nano Lett. 2001, 55, 6.
7. U. Simon, G. Schön, G. Schmid, Angew. Chemie Int. Ed. English 1993, 32, 250.
8. G. Schmid, R. Pugin, T. Sawitowski, Chem. Commun. 1999, 55, 1303.
9. M. Marcus, M. Andrews, Phys. Rev. B 1990, 42, 3312.
10. M. C. Farirbanks, R. E. Benfield, R. J. Newport, G. Schmid, Solid State Commun. 1990, 73, 431.
11. R. Benfield, D. Grandjean, J. Phys. Chem. B 2001, 105, 1961.
12. W. Vogel, B. Rosner, B. Tesche, J. Phys. Chem. 1993, 97, 11611.
13. Y. Pei, N. Shao, Y. Gao, X. Zeng, ACS Nano 2010, 4, 2009.
14. D. Rapoport, W. Vogel, J. Phys. Chem. B 1997, 101, 4175.
15. L. Wallenberg, J. Bovin, G. Schmid, Surf. Sci. 1985, 156, 256.
16. A. Crewe, J. Wall, J. Langmore, Science. 1970, 168, 1338.
17. S. Pennycook, Ultramicroscopy 1989, 30, 58.
18. R. F. Loane, P. Xu, J. Silcox, Ultramicroscopy 1992, 40, 121.
19. Z. Wang, Z. Li, S. Park, A. Abdela, Phys. Rev. B 2011, 84, 073408.
20. Z. W. Wang, O. Toikkanen, B. M. Quinn, R. E. Palmer, Small 2011, 7, 1542.
21. S. Van Aert, K. J. Batenburg, M. D. Rossell, R. Erni, G. Van Tendeloo, Nature 2011, 470, 374.
22. Z. Wang, R. Palmer, Nanoscale 2012, 4, 4947.
23. A. Engel, Ultramicroscopy 1978, 3, 273.
24. J. McBride, J. Treadway, L. C. Feldman, S. J. Pennycook, S. J. Rosenthal, Nano Lett. 2006, 6, 1496.
25. D. Ferrer, a Torres-Castro, X. Gao, S. Sepúlveda-Guzmán, U. Ortiz-Méndez, M. José-Yacamán, Nano Lett. 2007, 7, 1701.
26. P. M. Voyles, D. a Muller, J. L. Grazul, P. H. Citrin, H.-J. L. Gossmann, Nature 2002, 416, 826.
27. V. Altoe, F. Martin, A. Katan, M. Salmeron, S. Aloni, Nano Lett. 2012, 12, 1295.
28. P. Nellist, S. Pennycook, Science. 1996, 274, 2.
29. Z. Y. Li, N. P. Young, M. Di Vece, S. Palomba, R. E. Palmer, a L. Bleloch, B. C. Curley, R. L. Johnston, J. Jiang, J. Yuan, Nature 2008, 451, 46.
30. N. Young, Z. Li, Y. Chen, S. Palomba, Phys. Rev. Lett. 2008, 101, 246103.
31. Z. Wang, O. Toikkanen, F. Yin, J. Am. Chem. Soc. 2010, 132, 2854.
32. Z. W. Wang, R. E. Palmer, Nano Lett. 2012, 12, 91.
33. S. R. Plant, L. Cao, F. Yin, Z. W. Wang, R. E. Palmer, Nanoscale 2014, 6, 1258.
34. I. Garzón, K. Michaelian, M. Beltrán, a. Posada-Amarillas, P. Ordejón, E. Artacho, D. Sánchez-Portal, J. Soler, Phys. Rev. Lett. 1998, 81, 1600.
35. I. Garzón, J. Reyes-Nava, J. Rodríguez-Hernández, I. Sigal, M. Beltrán, K. Michaelian, Phys. Rev. B 2002, 66, 073403.
36. B. von Issendorff, R. E. Palmer, Rev. Sci. Instrum. 1999, 70, 4497.
37. S. Pratontep, P. Preece, C. Xirouchaki, R. E. Palmer, Phys. Rev. Lett. 2003, 90, 055503.
38. S. Pratontep, S. Carroll, Rev. Sci. Instrum. 2005, 76, 045103.
39. Y. Han, D. S. He, Y. Liu, S. Xie, T. Tsukuda, Z. Y. Li, Small 2012, 8, 2361.
40. C. Koch, PhD thesis, 5, 2002.
41. Z. Wang, R. Palmer, Phys. Rev. Lett. 2012, 108, 245502.
42. Z. W. Wang, R. E. Palmer, J. Phys. Conf. Ser. 2012, 371, 012010.
43. Z. W. Wang, R. E. Palmer, Nano Lett. 2012, 12, 5510.
44. L. Marks, Reports Prog. Phys. 1994, 57, 603.
45. D. B. Williams, C. B. Carter, Transmission Electron Microscopy—A Textbook for Materials Science, springer, NY, USA 2008.
46. P. D. Jadzinsky, G. Calero, C. J. Ackerson, D. a Bushnell, and R. D. Kornberg, Science, 2007, 318, 430–433.
47. O. Lopez-Acevedo and J. Akola, J. Phys. Chem. C, 2009, 144, 5035–5038.
48. R. Jin, Nanoscale, 2010, 2, 343–62.
49. D. Bahena and N. Bhattarai, J. Phys. Chem. Lett., 2013, 144.